Cell

Hsp90 Cochaperone Aha1 Downregulation Rescues Misfolding of CFTR in Cystic Fibrosis

Xiaodong Wang,[1,6,7] John Venable,[1,6] Paul LaPointe,[1,6] Darren M. Hutt,[1,6] Atanas V. Koulov,[1] Judith Coppinger,[1] Cemal Gurkan,[1] Wendy Kellner,[1] Jeanne Matteson,[1] Helen Plutner,[1] John R. Riordan,[5] Jeffery W. Kelly,[2,3] John R. Yates, III,[1,*] and William E. Balch[1,4,*]
[1] Department of Cell Biology
[2] Department of Chemistry
[3] The Skaggs Institute for Chemical Biology
[4] The Institute for Childhood and Neglected Disease
The Scripps Research Institute, 10550 North Torrey Pines Road, La Jolla, CA 92037, USA
[5] Department of Biochemistry and Biophysics, 5011 Thurston-Bowles Building, University of North Carolina, Chapel Hill, NC, 27510, USA
[6] These authors contributed equally to this work.
[7] Present address: Department of Pharmacology, Medical University of Ohio, Block Health Science Building, 3035 Arlington Avenue, Toledo, OH 43614, USA.
*Contact: jyates@scripps.edu (J.R.Y.), webalch@scripps.edu (W.E.B.)
DOI 10.1016/j.cell.2006.09.043

SUMMARY

The pathways that distinguish transport of folded and misfolded cargo through the exocytic (secretory) pathway of eukaryotic cells remain unknown. Using proteomics to assess global cystic fibrosis (CF) transmembrane conductance regulator (CFTR) protein interactions (the CFTR interactome), we show that Hsp90 cochaperones modulate Hsp90-dependent stability of CFTR protein folding in the endoplasmic reticulum (ER). Cell-surface rescue of the most common disease variant that is restricted to the ER, ΔF508, can be initiated by partial siRNA silencing of the Hsp90 cochaperone ATPase regulator Aha1. We propose that failure of ΔF508 to achieve an energetically favorable fold in response to the steady-state dynamics of the chaperone folding environment (the "chaperome") is responsible for the pathophysiology of CF. The activity of cargo-associated chaperome components may be a common mechanism regulating folding for ER exit, providing a general framework for correction of misfolding disease.

INTRODUCTION

A major challenge in cell biology is to understand the role of protein energetics and chaperone function in the folding of cargo for export from the endoplasmic reticulum (ER) (Kelly and Balch, 2006; Sekijima et al., 2005). The ER is a specialized folding environment in which nearly one-third of the proteins coded for by the eukaryotic genome are translocated and folded as either lumenal secreted proteins or transmembrane proteins. Proteins are exported from the ER by the coatomer complex II (COPII) machinery, which generates transport vesicles for delivery of cargo to the Golgi (Lee et al., 2004; Stagg et al., 2006; Gurkan et al., 2006). The metabolic basis for the function of the abundant ER lumenal and cytosolic chaperone machineries remains to be fully elucidated. These ER-associated folding (ERAF) pathways are also coordinated with ER-associated degradation (ERAD) pathways whereby misfolded proteins are targeted for retrotranslocation to the cytosolic proteasome system (Young et al., 2003).

Numerous misfolding diseases occur in which variants of either lumenal or transmembrane cargo do not fold properly, fail to engage the COPII export machinery, and are degraded in the ER, resulting in loss-of-function phenotypes. We have recently demonstrated the importance of both the kinetic and thermodynamic properties of the protein fold in defining a minimal energetic threshold required for export of cargo responsible for misfolding disease (Sekijima et al., 2005). These results raised the possibility that the chaperone environment may play a critical role in establishing the export threshold whereby energetically destabilized (misfolded) cargo fails to be exported efficiently.

Cystic fibrosis (CF) is an inherited childhood disease primarily triggered by defective folding and export of CFTR from the ER (Riordan, 2005). The cystic fibrosis transmembrane conductance regulator (CFTR) is a multidomain cAMP-regulated chloride channel found in the apical membrane of polarized epithelia lining many tissues. CFTR

consists of two transmembrane domains (TMD1 and 2) separated biosynthetically by cytosol-oriented N- and C-terminal domains and the NBD1, R, and NBD2 domains that regulate channel conductance. Transport of CFTR involves both lumenal and cytosolic chaperones that facilitate folding and export from the ER (Amaral, 2006; Riordan, 2005), as well as adaptor proteins that direct trafficking from the *trans*-Golgi and recycling through endocytic pathways to maintain the proper level of chloride-channel activity at the cell surface (Guggino and Stanton, 2006). In addition, a number of proteins regulate CFTR channel conductance through both cAMP and G protein-coupled signaling mechanisms, and a variety of effectors are critical to allow CFTR to regulate other ion transporters involved in Na^{2+} and HCO^{3-} transport to maintain normal cellular ion balance in tissues (Guggino and Stanton, 2006). The full extent of these protein interactions and their importance for CFTR function in tissue remain to be elucidated.

Over 90% of CF patients carry at least one allele of the Phe508 deletion (ΔF508 CFTR) in the cytosolic NBD1 ATP-binding domain that leads to severe forms of disease. Loss of Phe508 disrupts the folding pathway of CFTR in the ER (Qu et al., 1997; Riordan, 2005). In vitro biochemical and biophysical experiments with purified NBD1 have demonstrated that the thermodynamic stability of the wild-type and mutant domain is similar, a result consistent with recent structural studies in which both wild-type and ΔF508 are found to have nearly identical folds (Lewis et al., 2004). In contrast, the folding of ΔF508 NBD1 is kinetically impaired (Qu et al., 1997). As a consequence of this energetic defect in folding, ΔF508 fails to achieve a wild-type fold in the ER, fails to engage the COPII ER export machinery (Wang et al., 2004), and is targeted for ERAD (Nishikawa et al., 2005).

Chaperone components that are currently thought to significantly affect CFTR ERAF pathways include calnexin, found in the lumen of the ER, as well as the cytosolic chaperone complexes Hsc-Hsp40/70 and Hsp90 (Amaral, 2006; Riordan, 2005). The specific mechanism (or mechanisms) by which the Phe508 deletion disrupts folding of CFTR remains a topic of considerable debate but likely involves the Hsc-Hsp70 pathway and its coregulators. Past biochemical studies suggest that these chaperones function in co- and posttranslational processes to help integrate the folds of TMD1 and 2 and the cytosolic NBD1, R, and NBD2 domains that could be disrupted by the mutation. In addition, the Hsp90 inhibitor geldanamycin (GA) has been shown to destabilize wild-type CFTR during nascent synthesis (Loo et al., 1998), targeting the protein for rapid degradation. Hsp90-dependent modification of the folding properties of a variety of client proteins is regulated by cyclical interactions with a variety of different cochaperones. These cochaperones have been studied extensively for their roles in modulating Hsp90-client interactions such as found for steroid hormone receptors (SHRs) and signaling kinases (Wegele et al., 2004). Thus, it is apparent that Hsp90 and its cochaperones may also play important but unknown roles in folding for export. Although the loss of Phe508 kinetically disrupts stability in the ER, the destabilized protein still retains significant chloride-channel conductance (Amaral, 2006). Such results suggest that insight into the molecular machinery directing folding and export could play an important role in both understanding the molecular basis for disease and achieving correction by promoting folding and transport of ΔF508 to the cell surface.

Herein, we have applied mass spectrometry through use of multidimensional protein identification technology (MudPIT) (Washburn et al., 2001) to begin to define the global protein interactions (the CFTR interactome) required for folding, trafficking, and function of CFTR in the exocytic and endocytic pathways. The interactome reveals a cohort of known and unknown regulators and effectors in ER and post-ER compartments that guide CFTR function. Given the importance of identifying the critical interactions defective in ΔF508 disease, we have focused in this study on the key differences in the wild-type and ΔF508 proteomes affecting ER export. Consistent with previous studies, we find that both wild-type and ΔF508 CFTR have robust interactions with lumenal chaperones including calnexin and the cytosolic chaperone machineries Hsc-Hsp70 and 90. We now show that the cochaperone interactions of ΔF508 and wild-type CFTR with Hsp90 differ, suggesting that the ΔF508 is kinetically restricted to a folding intermediate in the ER. Strikingly, modest siRNA reduction of the Hsp90 cochaperone Aha1 rescues trafficking of ΔF508 to the cell surface and restores channel function, suggesting that the chaperone pool governing the folding of the cytosolic domains of ΔF508 can be adjusted physiologically to achieve export. Our results are consistent with the view that the cellular chaperone pool (the "chaperome") does not simply prevent aggregation but can also contribute to local folding environments (Albanese et al., 2006), controlling the success or failure of the protein fold for function and export. We raise the possibility that rescue of misfolding diseases may be achievable through understanding the cargo-specific roles of chaperome components facilitating stabilization of energetically unstable folds found in the wide range of polymorphisms and mutations observed in health and disease. By rescuing the protein fold, we simultaneously correct the many downstream interactions that are contributing to disease (Kelly and Balch, 2006).

RESULTS

The CFTR Interactome

To define global protein interactions involved in CFTR trafficking and function in the exocytic and endocytic pathways, CFTR-containing protein complexes were immunoisolated from heterologous lung and intestine cell lines expressing wild-type CFTR and were protease digested, and the composition of the peptide mixture was determined using MudPIT (Washburn et al., 2001). Proteins identified in the CFTR immunoprecipitates that were not

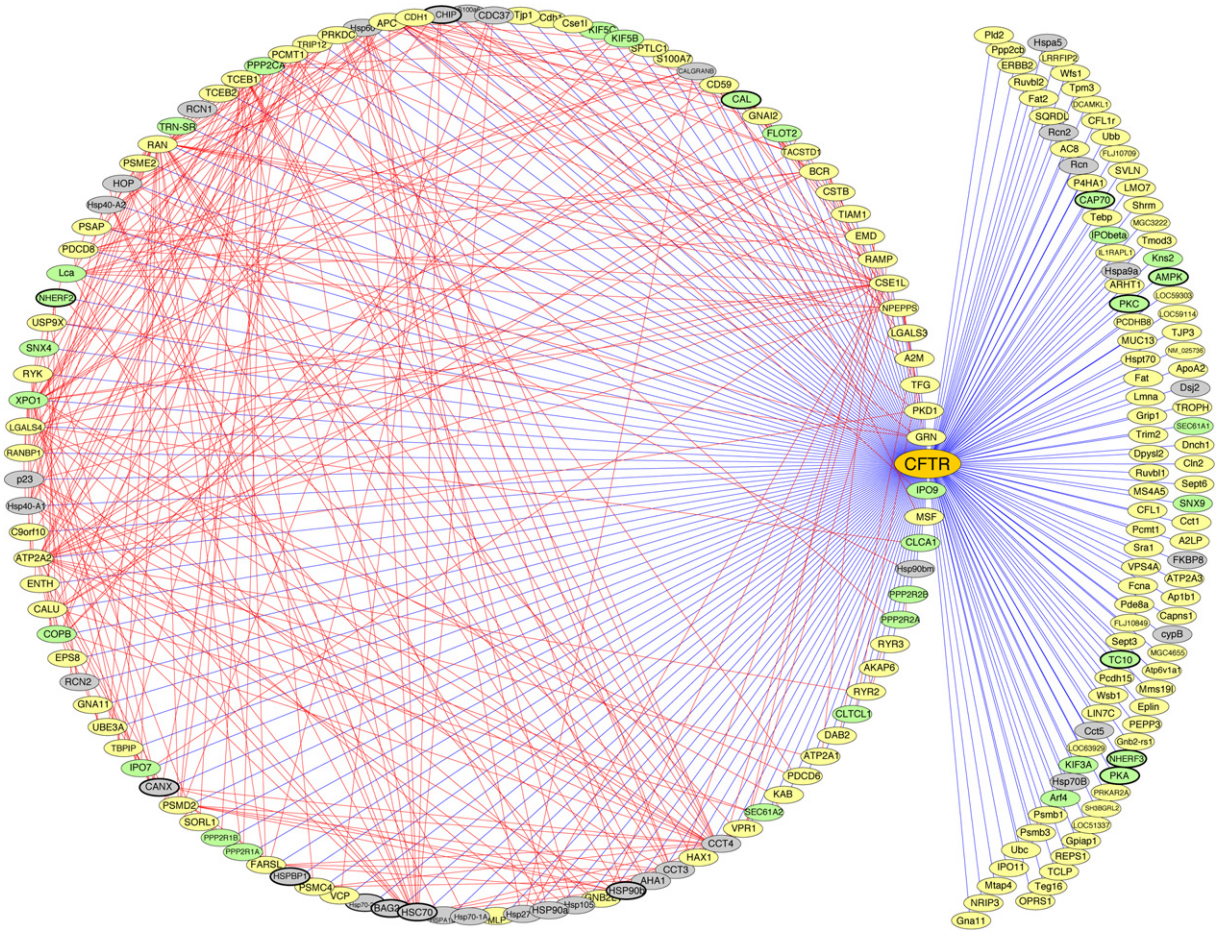

Figure 1. The CFTR Interactome

All components comprising the CFTR interactome are depicted as nodes (ovals) in the network. Components identified in previous studies as CFTR interactors are highlighted with bold lines surrounding the ovals. Straight blue lines are edges in the network that show direct or indirect protein interactions between CFTR and the indicated component identified by MudPIT. Straight red lines illustrate edges that define interactions based on the BIND (http://www.bind.ca/Action) and DIP (http://dip.doe-mbi.ucla.edu/) protein interaction databases and the Tmm coexpression database (http://microarray.cpmc.columbia.edu/tmm/), which were accessed using the Cytoscape platform (http://www.cytoscape.org/). Proteins involved in folding and export from the ER are illustrated as gray nodes; green nodes highlight protein interactions involved in post-ER trafficking and activity. Yellow nodes indicate interactors with unknown function. See the Supplemental Discussion for a more complete description of proteins defined by green and yellow nodes. The network also includes proteins previously demonstrated to modulate CFTR folding and function that were not detected in the cell lines analyzed in the current study (Amaral, 2006; Guggino and Stanton, 2006).

observed in control immunoprecipitates from cell lines lacking CFTR or in immunoprecipitates prepared from CFTR-expressing cell lines using nonspecific antibody provide us with a comprehensive network of CFTR-interacting components (Figure 1; see also Tables S1–S7 in the Supplemental Data available with this article online), which we refer to as the CFTR interactome. Whereas high sequence and spectra coverage of interactors likely reflect a strong, persistent interaction with CFTR (Liu et al., 2004), interactors identified with high fidelity using at least two spectra either reflect molecules that have indirect, weak, or transient interactions or reflect tissue-specific differences in trafficking, function, and regulation. Proteins comprising the CFTR interactome belong to a variety of functional groups that include components required for folding and export from in the ER (Figure 1, gray), those that have functional relevance for trafficking and activity at the cell surface (Figure 1, green) (Guggino and Stanton, 2006), and proteins that have as yet to be defined roles with respect to their potential role in CFTR folding and function (Figure 1, yellow). Proteins highlighted in green are described in further detail in the Supplemental Discussion. In addition to new interactors, components previously documented to interact with CFTR (Figure 1, bolded ovals) validate the current shotgun proteomics approach to define a comprehensive database for addressing CFTR function.

The critical step for understanding the most common form of CF is to define the basis for the loss of export of ΔF508 from the ER that reflects a key step (or steps) in

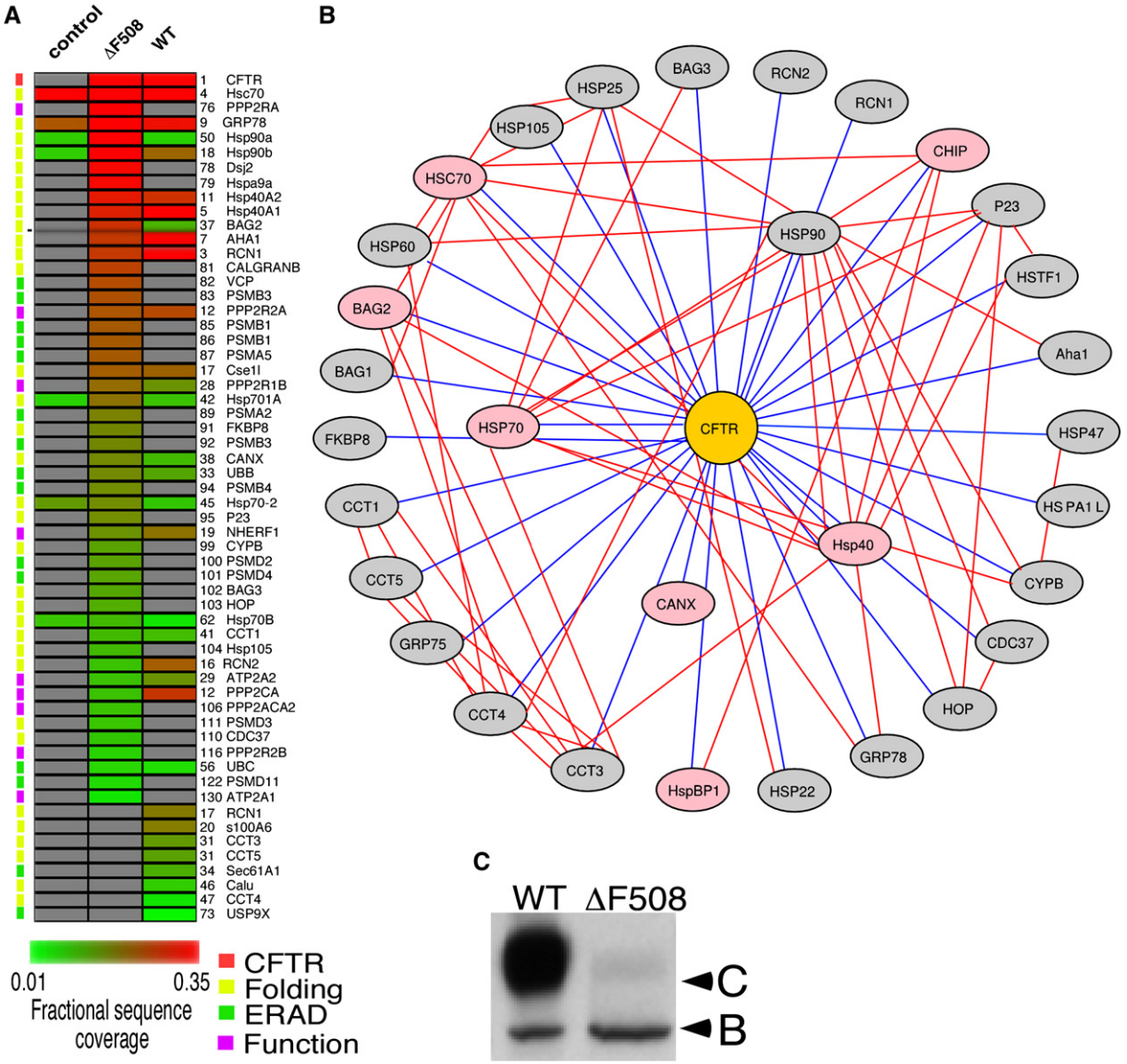

Figure 2. The ER Chaperone Network

(A) Proteins involved in folding (yellow) and degradation (green) in BHK cells not expressing CFTR (control) or those expressing either ΔF508 or wild-type CFTR are shown as an array and are arranged in order of fractional sequence coverage by mass spectrometry (bar at base of array). Gray indicates absence of the protein in the proteome data set. Chaperone components observed in the control were routinely recovered with low spectral coverage when compared to ΔF508 CFTR, with the exception of Hsc70, which is detected in most immunoprecipitates analyzed by MudPIT given its very high cellular abundance. Proteins thought to be involved in CFTR function (purple) are associated with ΔF508 in the ER, suggesting a possible role in folding or export. A full description of each protein identified by the number and abbreviation listed to the right side of the array can be found in the complete data set in Table S2.

(B) Network view of the components involved in CFTR folding (see Tables S1 and S2 for full descriptions). Components demonstrated previously to facilitate folding are shown in pink. Blue lines indicate potential direct or indirect interactions with CFTR; red lines indicate confirmed physical interactions between components based on data from the HPRD (http://www.hprd.org/), IntAct (http://www.ebi.ac.uk/intact/site/), BIND, and DIP.

(C) SDS-PAGE immunoblot showing the typical steady-state levels of bands B and C observed in wild-type and ΔF508 CFTR-expressing cells used in the present study.

protein folding events that direct ER export through either ERAF (Sekijima et al., 2005) or degradation pathways. Consistent with these results, the proteomes of wild-type CFTR-expressing cells showed robust linkage based on total spectra recovered to calnexin and the Hsc-Hsp40/70 and Hsp90 cytosolic "core" chaperones (Figure 2B, inner circle of components; Table 1; Table S1). To identify components in the interactome that may be involved in the failure of ΔF508 to couple to the ER folding and export machinery, likely a step common to all cell

Table 1. The CFTR ER-Associated Folding Proteome

		ΔF508 CFTR			WT CFTR		
RefSeq AC	Protein Name	Sequence Coverage (%)	Unique Spectra	Total Spectra	Sequence Coverage (%)	Unique Spectra	Total Spectra
NM_000492	CFTR	57	229	2481	60	333	4172
NM_024351	Hsc70	60	66	369	48	39	132
NM_022310	GRP78[a]	40	30	85	33	17	37
NM_021979	Hsp70-2	16	23	57	8	7	17
NM_001746	calnexin[a]	16	13	52	10	4	7
NM_008302	Hsp90β	36	24	49	21	11	18
NM_010481	GRP75	34	23	40			
NM_005348	Hsp90α	39	24	37	6	4	5
NM_022934	DnaJ-like protein	34	11	35			
NM_001539	Hsp40-A1 (Hdj2)	31	10	33	40	13	25
NM_005345	Hsp70-1A	19	12	20	8	4	6
NM_004282	BAG-2	28	7	20	10	2	2
NM_005880	Hsp40-A2 (Hdj3)	32	9	19	28	6	16
NM_002155	Hsp70B′	10	8	14	3	3	5
NM_013559	Hsp105	10	5	6			
NM_013686	TCP1	10	3	5	9	3	5
NM_010223	FKBP8	17	4	5			
NM_013863	BAG-3	12	4	5			
NM_016737	Hop	11	4	4			
NM_016742	Cdc37	8	2	3			
NM_000942	cyclophilin B[a]	13	2	2			
NM_006601	p23	16	2	2			
NM_012111	Aha1	15	7	15	34	10	20
NM_009037	reticulocalbin[a]	27	5	8	50	14	19
NM_011992	reticulocalbin 2[a]	9	3	4	22	6	12
NM_001219	calumenin[a]				7	3	3

Indicated are the interacting proteins in BHK cells, their percentage sequence coverage, number of unique spectra, and number of total spectra as detected by mass spectrometry in cell lines examined (Figure 1).
[a] ER lumenal chaperones.

types, we compared the CFTR-specific proteomes immunoprecipitated from matched BHK cell lines heterologously expressing wild-type or ΔF508 CFTR; the parent BHK cell line lacking CFTR was used as a negative control for nonspecific interactions (Figure 2A). At physiological temperature (37°C), wild-type CFTR is principally in the band C Golgi-processed glycoform found at the cell surface, with the band B ER-associated core-glycosylated glycoform comprising <10%–20% of the total CFTR pool (Figure 2C). In contrast, in cells expressing ΔF508 at 37°C, generally only 5%–20% of the protein (reflecting cell type and growth conditions) can be detected in band C due to significantly reduced stability and folding for export. Thus, ΔF508 is largely restricted to the immature core-glycosylated band B ER glycoform (Figure 2C), where it is efficiently targeted for ERAD.

Like wild-type CFTR, ΔF508 showed strong interactions with the core lumenal chaperone calnexin and Hsc-Hsp40/70 and Hsp90 cytosolic core components. Regulatory interactions by cochaperones may be difficult to capture in proteome experiments in which the wild-type CFTR folding population may be only transiently populated and therefore nonabundant (Kelly and Balch, 2006). In contrast, because previous studies have suggested that folding of ΔF508 is kinetically impaired (Qu et al., 1997), components recovered in the ΔF508 interactome may include those associated with a kinetically impaired folding intermediate (or intermediates) sensitive to the Phe508

deletion. Consistent with this prediction, we not only detected an increase in spectra and sequence coverage of core chaperone components (Figure 2A; Table 1) but also detected a number of cochaperone components in the ΔF508 ER interactome that were not generally recovered in the wild-type proteome (Figure 2B, outer circle of components; Table 1). Cytosolic chaperone coregulators of Hsc-Hsp70 detected included BAG-2/3, involved in the degradation of CFTR, and Hsp105, which modulates Hsc70 function (Amaral, 2006). Strikingly, we noted a number of Hsp90 cochaperones. These included, for example, the Hsc-Hsp70/Hsp90 organizing protein (HOP), p23, Cdc37, the immunophilin FKBP8, and Aha1, an ATPase regulator of Hsp90. Thus, the CFTR interactome reveals important physiological changes in the chaperone binding to misfolded proteins that need to be understood.

Hsp90 Cochaperones Can Modulate CFTR Stability in the ER

To begin to define the role of Hsp90 in folding and export of ΔF508 CFTR, we used siRNA and transient transfection to control the level of protein expression of select Hsp90 cochaperones including p23 (Figure 3) and the immunophilin FKBP8 (Figure 4), which have been previously documented to regulate ATP-dependent folding steps in the cyclic Hsp90-client interaction pathway (Wegele et al., 2004). Following initial recognition of a folding client molecule such as CFTR by Hsc-Hsp40/70, the ubiquitous cochaperone HOP links the nascent Hsc-Hsp40/70-client complex to Hsp90 in the ADP state. Subsequently, the cochaperone regulator p23, in the presence of ATP, displaces Hsc-Hsp40/70 and HOP to form the mature Hsp90-p23-client complex in the ATP-bound state. The cycling of Hsp90-client chaperone complexes containing p23 are further regulated by immunophilins.

We first examined the role of the cochaperone regulator p23 in HEK293 cells stably expressing ΔF508. In each experiment, the total amount of band B or C recovered was standardized using SDS-PAGE by loading identical levels of total protein in each lane, and the immunoblot was developed under identical conditions (see Supplemental Experimental Procedures). siRNA reduction of p23 levels by ~70% resulted in a comparable (60%–70%) reduction in the steady-state pools of both the band B ER glycoform and the small pool of the band C cell-surface glycoform when compared to the scrambled mock control (Figure 3A, left panel). Conversely, overexpression (3- to 5-fold) partially stabilized band B but did not result in a significant increase in band C (Figure 3A, right panel). siRNA reduction of p23 had a similar effect on stability of both band B and C wild-type CFTR in HEK293 cells (data not shown). Thus, as has been observed in numerous other client-chaperone interactions, the steady-state level of p23 in the general chaperone pool of the cell affects the overall folding properties of CFTR with respect to Hsp90 function.

Because ΔF508 CFTR is a temperature-sensitive folding mutant, incubation of cells at the permissive temperature (30°) instead of 37°C provides a more energetically favorable folding environment leading to significant levels of cell-surface-localized ΔF508. At steady state (15 hr post temperature shift from 37°C to 30°C), 40%–50% of the total ΔF508 pool in HEK293 cells is typically found in band C (Figure 3B, left panel). This likely reflects the fact that, at reduced temperature, the ΔF508 folding pathway is more stabilized. Notably, even at the permissive folding temperature (30°C), siRNA reduction of p23 resulted in a significant decrease in the stability of band B and processing to band C (Figure 3B, left panel) as was observed

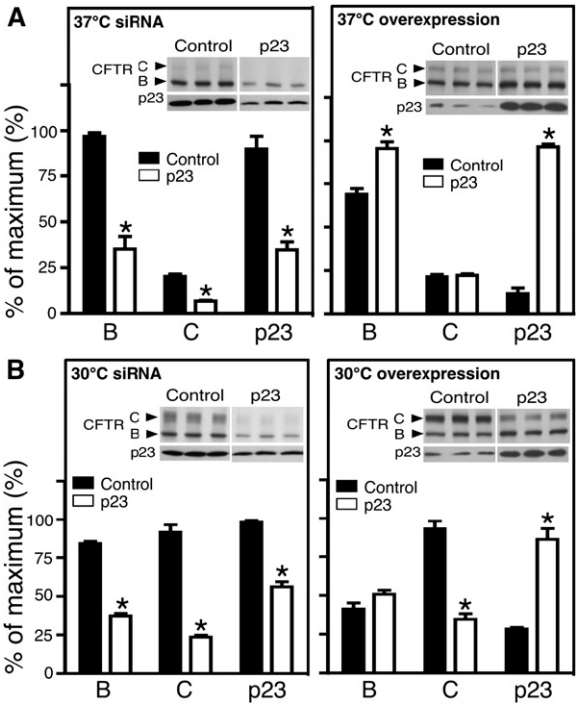

Figure 3. Effect of the Hsp90 Cochaperone p23 on Folding and Export of ΔF508 from the ER

(A) Human siRNA to p23 (left panel) was used to reduce expression of the indicated protein at 37°C as described in the Supplemental Experimental Procedures. The steady-state pool of band B (ER glycoform) and band C (cell-surface glycoform) was determined using immunoblotting as described in the Supplemental Experimental Procedures. Scrambled siRNA was used as a control. Human cDNA to p23 (right panel) was used to overexpress the indicated protein at 37°C as described in the Supplemental Experimental Procedures. The steady-state pools of bands B and C were determined using immunoblotting. In the inset, a representative immunoblot illustrates experimental variation between triplicate samples. In this and all other figures, error bars represent standard error of the mean.

(B) Conditions were as described for (A), except that cells were incubated at the permissive temperature (30°) to promote folding and export from the ER as described in the Supplemental Experimental Procedures. *$p \leq 0.05$ by unpaired, two-tailed t test (triplicate samples). Experiments were repeated independently in triplicate at least three times, with representative results shown. All lanes were loaded with equivalent levels of total protein, and the immunoblot containing both the control (scrambled) and siRNA/cDNA was developed identically and quantified as described in the Supplemental Experimental Procedures.

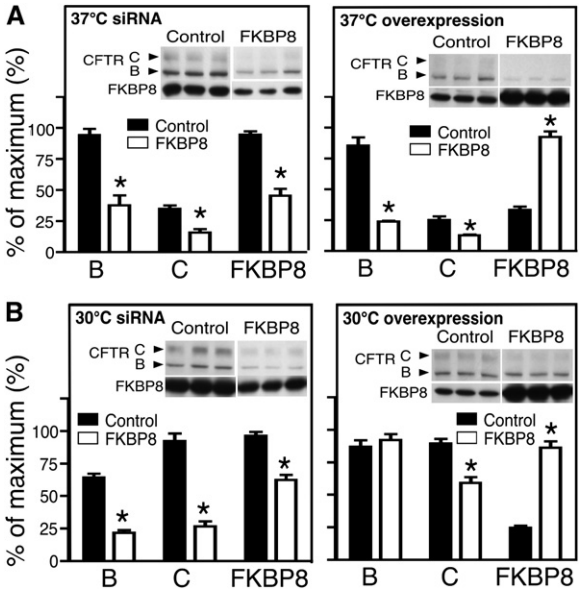

Figure 4. Effect of the Hsp90 Cochaperone FKBP8 on Folding and Export of ΔF508 from the ER

(A) Human siRNA to FKBP8 (left panel) was used to reduce expression of the indicated protein at 37°C. The steady-state pool of band B (ER glycoform) and band C (cell-surface glycoform) was determined using immunoblotting. Scrambled siRNA was used as a control. Human cDNA to FKBP8 (right panel) was used to overexpress the indicated protein at 37°C. The steady-state pools of bands B and C were determined using immunoblotting.

(B) Conditions were as described for (A), except that cells were incubated at the permissive temperature (30°) to promote folding and export from the ER. *$p \leq 0.05$ by unpaired, two-tailed t test (triplicate samples). Experiments were repeated independently in triplicate at least three times, with representative results shown.

at 37°C. Interestingly, at 30°C, overexpression had no effect on stabilization of band B as observed at 37°C but markedly prevented processing to band C (Figure 3B, right panel). Thus, the folding properties of 37°C and temperature-corrected ΔF508 show different dynamics with respect to the Hsp90 cochaperone machinery. The dominant-negative effect of p23 overexpression on CFTR transport and conversion to band C may reflect what has been observed for other Hsp90-dependent signaling pathways where signaling is inhibited in response to excessive stabilization of the mature client complex (Pratt and Toft, 2003). One possibility is that a block in Hsp90 cycling in the presence of excess p23 could inhibit access of CFTR to the ER export machinery. Thus, p23 is a modular component that can affect ΔF508 folding, yet it does not appear to promote access of ΔF508 to the ER export machinery.

Although we were unable to identify FKBP52, an immunophilin involved in SHR folding (Pratt and Toft, 2003), in the ΔF508 CFTR interactome, we detected the family member FKBP8 (Nielsen et al., 2004; Shirane and Nakayama, 2003). FKBP8 is a membrane-associated immunophilin that has been reported to be localized to both the mitochondria and the ER. Consistent with these results, we have found that FKBP8 has substantial overlap with the ER marker protein calnexin (data not shown). Similar to the effect of p23 siRNA, we observed significant destabilization of ΔF508 in response to siRNA reduction of FKBP8 at 37°C (Figure 4A, left panel). Interestingly, overexpression at 37°C also destabilized CFTR (Figure 4A, right panel), raising the possibility that FKBP8 function and expression are tied to the steady-state concentration of Hsp90 to insure optimal performance of the CFTR-specific Hsp90-client folding pathway. siRNA reduction of FKBP8 expression also reduced (to 30%–40%) the stability of ΔF508 CFTR at the permissive folding temperature (30°C), with a corresponding reduction in the level of band C (~50%) (Figure 4B, left panel). In contrast, overexpression at 30°C had only a modest effect on stability and interfered with processing to band C (Figure 4B, right panel). Thus, like p23, interaction of the immunophilin FKBP8 with the Hsp90-CFTR client complex appears to differentially regulate the folding pathway, reflecting the concentration of the chaperone, yet fails to rescue export at 37°C.

In summary, the combined analysis of under- or overexpression of p23 and FKBP8 is consistent with an interpretation in which these cochaperones can act as folding modulators that influence ΔF508 stability in the ER yet do not participate in steps leading to delivery of a folded form of CFTR to the ER export machinery.

Aha1 Downregulation Rescues Delivery of ΔF508 to the Cell Surface

A recently recognized member of the Hsp90 cochaperone family is Aha1. Aha1 binds the middle domain of Hsp90 and is proposed to function as an ATPase-activating protein that competes with p23 and other cochaperones for Hsp90 binding (Harst et al., 2005; Lotz et al., 2003; Meyer, 2004; Panaretou et al., 2002). siRNA reduction of the endogenous level of Aha1 in HEK293 cells by 50%–70% resulted in a marked 3- to 4-fold stabilization of ΔF508 band B (Figure 5A, upper left panel). An even more pronounced stabilization (4- to 5-fold) was observed at 30°C (Figure 5A, lower left panel). Strikingly, at both 37°C and 30°C, stabilization was accompanied by a corresponding increase in band C reflecting significant cell-surface delivery (Figure 5A, left panels), a result not observed with the other cochaperones examined (Figure 3 and Figure 4). The rescued band C was resistant to processing by endoglycosidase H (Figure S1), a hallmark of transport through the Golgi complex. In contrast to the effects of siRNA, overexpression (~4-fold) of Aha1 in HEK293 cells expressing ΔF508 significantly destabilized band B at both 37°C (~60%) and 30°C (>90%) with a corresponding loss of processing to band C (Figure 5A, right panels).

Because HEK293 cells do not normally express ΔF508 and therefore may represent a special condition that is uniquely sensitive to the level of Aha1 activity, we examined the effect of Aha1 siRNA at 37°C in a lung cell line (CFBE41o−) that expresses ΔF508. Similar to the result

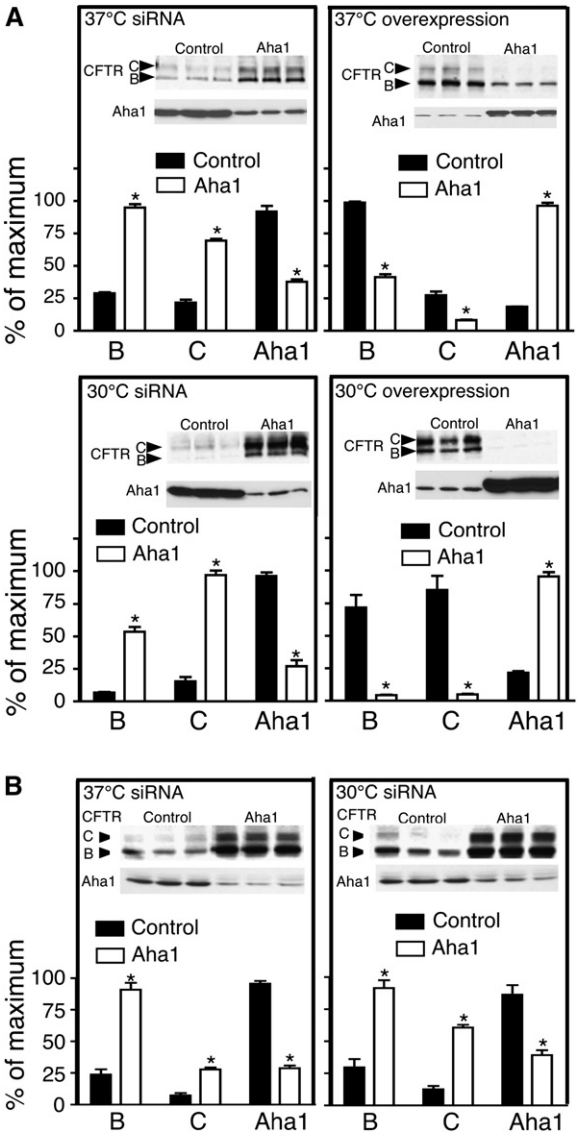

Figure 5. ΔF508 Export to the Cell Surface in HEK293 Cells Can Be Rescued by Downregulation of Aha1

(A) Human Aha1 siRNA (left panels) or human Aha1 cDNA (right panels) was used to reduce or overexpress, respectively, Aha1 in HEK293 cells expressing ΔF508 at 37°C (upper panels) or 30°C (lower panels), and the steady-state pools of bands B and C were determined using immunoblotting as described in Figure 2.

(B) Human Aha1 siRNA was used to reduce Aha1 expression in CFBE41o− cells expressing ΔF508 at 37°C (left panel) or 30°C (right panel), and the steady-state pools of bands B and C were determined using immunoblotting as described in Figure 2. *$p \leq 0.05$ by unpaired, two-tailed t test (triplicate samples). Representative results are shown in triplicate from four independent experiments.

observed in HEK293 cells, reduction of Aha1 resulted in stabilization of band B (~4-fold) compared to the scrambled control, with a corresponding 4- to 5-fold increase of band C either at 37°C (Figure 5B, left panel) or 30°C (Figure 5B, right panel). This level was even greater than that typically observed in the corrected CFBE41o− cell line (HBE) that expresses wild-type CFTR.

Using pulse-chase analysis to analyze the short-term effects of overexpression of Aha1 (~4-fold), we observed a significant decrease in the stability of band B in both wild-type and ΔF508-expressing cells (Figure S2), indicating the general importance of Aha1 in regulating Hsp90-dependent folding of CFTR. In contrast, no effect of Aha1 siRNA (70% knockdown) was observed on the short-term synthesis or stabilization of wild-type CFTR in HBE cells (Figure S3, upper panel) or on the steady-state cell-surface levels of band C (data not shown). Using a similar short pulse-chase protocol, siRNA significantly stabilized the nascent pool of ΔF508 in CFBE41o− cells (Figure S3, lower panel), although efficient processing to band C was not apparent during the chase as was observed for wild-type CFTR (Figure S3). These results are consistent with the interpretation that the pulse-labeled ΔF508 equilibrates with the unlabeled pool of ΔF508 that has accumulated in the ER during siRNA treatment, interfering with detection of radiolabeled processing intermediates (Figure 5B). Thus, the stabilization of band B and recovery of ΔF508 band C in response to reduced levels of Aha1 suggest that Aha1 activity may facilitate folding dynamics that favor stability and coupling of ΔF508 to the ER export machinery.

Hsp90 Binding to CFTR Is Responsive to Aha1 Activity

To determine the effect of Aha1 knockdown on the interaction of ΔF508 with Hsp90, we analyzed the recovery of Hsp90 bound to CFTR following treatment of cells with Aha1 siRNA. Cells expressing ΔF508 at 37°C were incubated in presence of scrambled or Aha1 siRNA. Cells were harvested, CFTR was immunoprecipitated, and the amount of Hsp90 associated with ΔF508 was quantitated by immunoblotting. Under conditions where we observed an ~60% knockdown of Aha1 (Figure 6A, right panel), when we analyzed the ratio of Hsp90 to CFTR recovered in the immunoprecipitate to determine the relative amount of Hsp90 bound to CFTR under control or knockdown conditions, we observed a 50%–60% decrease of bound Hsp90 at reduced levels of Aha1 (Figure 6A, left panel). In contrast, we detected no change in the cellular levels of calnexin, BiP, Hsp40, Hsc-Hsp70, Hsp90, HOP, FKBP8, and p23 compared to the scrambled control under these conditions (see Figure S4), suggesting that a reduction in Aha1 alters the steady-state pool of ΔF508 associated with Hsp90 in the ER. This result is consistent with the observation that Hsp90 and Hsp90 cochaperone recovery in the CFTR wild-type interactome is reduced relative to the ΔF508 interactome despite comparable levels of band B (Figure 2; Table 1). The combined results raise the possibility that, by lowering the level of the Aha1 cochaperone regulator, we modify the kinetic interactions of ΔF508 with Hsp90 to facilitate more efficient progression through the folding pathway to favor export.

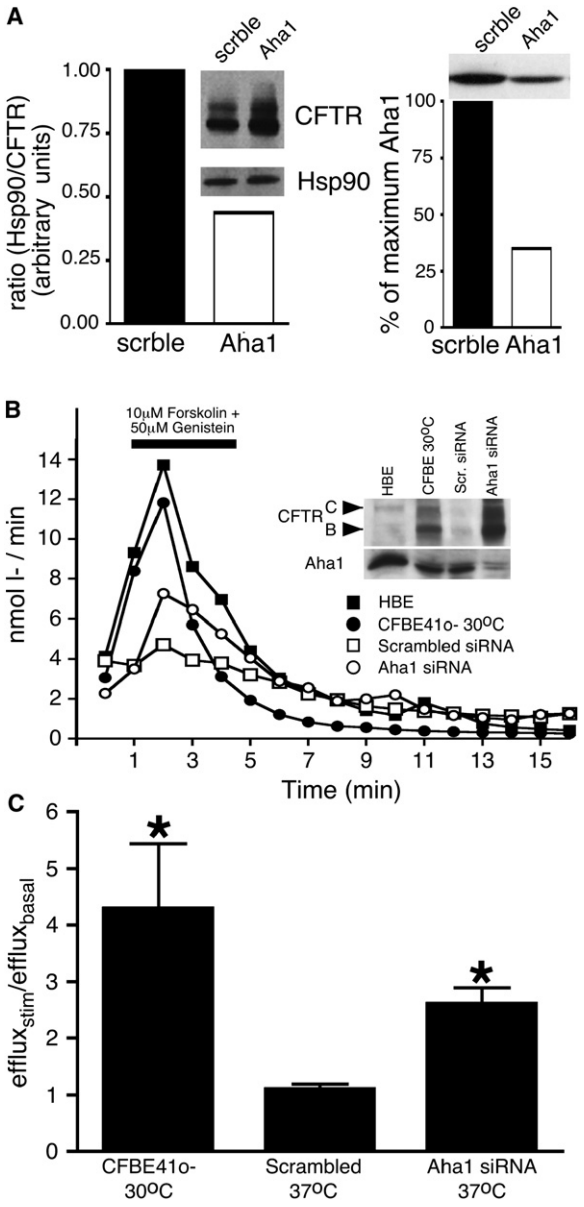

Figure 6. Effect of siRNA Aha1 on Hsp90 and Iodide Efflux

(A) HEK293 cells expressing ΔF508 at 37°C were incubated in the absence or presence of Aha1 siRNA as described in Figure 2. Cells were harvested, CFTR was immunoprecipitated, and the amount of Hsp90 recovered with ΔF508 was quantitated by immunoblotting. Ratio of Hsp90 to CFTR recovered in the immunoprecipitate is shown in the left panel; fraction of Aha1 remaining in cells following Aha1 siRNA treatment compared to scrambled control is shown in the right panel. (B) Iodide efflux (see Supplemental Experimental Procedures) was monitored in HBE cells expressing wild-type CFTR (■) or in ΔF508-expressing CFBE41o− cells that had been incubated at 37°C or, where indicated, at the permissive temperature of 30°C (final 15 hr) (●) or transfected with Aha1 (○) or scrambled (control) (□) siRNA. CFTR channels were activated by addition of 10 μM forskolin and 50 μM genistein over a 4 min period starting at 1 min and subsequently washed out with efflux buffer. The effect of temperature shift and siRNA on CFTR maturation (band B to band C glycoforms) and Aha1 stability is shown in the inset.

Aha 1 siRNA Restores Halide Conductance to CFBE41o− Cells Expressing ΔF508

While processing to the endo H-resistant band C glycoform is a hallmark of transport from the ER to the *cis*-/medial Golgi compartments, there remained the possibility that the rescued protein was trapped in late *trans*-Golgi or endocytic compartments, reflecting a potential contribution (or contributions) of the Phe508 deletion to abnormal sorting in post-ER pathways (Figure 1B) (Guggino and Stanton, 2006). To test for this possibility, CFBE41o− cells expressing ΔF508 were treated with Aha1 siRNA, and surface halide conductance was measured using an iodide efflux assay. As a positive control, we examined the halide conductance of the corrected HBE cell line expressing wild-type CFTR and temperature-corrected CFBE41o− cells. Treatment of the CFBE41o− cell line with Aha1 siRNA resulted in ~70%–80% knockdown of endogenous Aha1, leading to stabilization of ΔF508 band B and C at levels ~1.5-fold greater than the 30°C temperature-corrected control and a 4-fold stabilization of band B over the scrambled siRNA-treated cells (Figure 6B, inset). Whereas HBE cells showed strong halide conductance, no conductance was detected in control CFBE41o− cells that were treated with scrambled siRNA (Figure 6B). Shift of CFBE41o− to 30°C resulted in recovery of 80%–90% of the conductance observed in HBE cells (Figure 6B). Strikingly, CFBE41o− cells treated with Aha1, but not scrambled, siRNA showed on average from multiple experiments a 50% recovery of halide conductance compared to that observed in temperature-corrected cells (Figure 6C). This was not a statistically significant difference from that observed for the control 30°C temperature-shift value (Figure 6C). The ~2-fold higher level of band C observed in response to Aha1 siRNA relative to that observed in the temperature-corrected control (Figure 6B, inset) suggests either that the channel activity of temperature-corrected (30°C) ΔF508 is more responsive to cAMP stimulation than that of Aha1-corrected CFTR at 37°C or that the Aha1-corrected CFTR occupies, in part, endosomal compartments that are not accessible to the cell surface for halide conductance. The latter interpretation is consistent with the altered endocytic trafficking pathways encumbered by temperature-corrected ΔF508 when shifted to 37°C following delivery to the cell surface. It is now apparent that modulation of the Hsp90-client interaction in the ER through alteration of cochaperone pools can achieve functional rescue of CFTR. Whether manipulation of Aha1 to effect

(C) The ratio of halide conductance prior to addition of forskolin/genistein (0 min) and at 2 min, the peak period of halide flux. *$p \leq 0.05$ by unpaired, two-tailed t test (triplicate samples) between the temperature-corrected (first lane) and siRNA-treated (third lane) CFBE41o− cells compared to the scrambled siRNA-treated control (second lane). There was no statistically significant difference between halide conductance for temperature-corrected (first lane) and siRNA-treated CFBE41o− cells (third lane) ($p = 0.2$). Experiments were repeated independently at least three times, with representative results shown.

rescue of ΔF508 export will also alter in a more global way other Hsp90-sensitive folding pathways remains to be explored. Modest alteration to partially or fully correct destabilized folds may have little impact on normal cellular function given the inherent energetic stability of the wild-type fold (Kelly and Balch, 2006).

DISCUSSION

We have taken a systems biology approach aided by the sensitivity of MudPIT proteomics to identify transient interactions that contribute to CFTR folding, trafficking, and regulatory pathways—the CFTR interactome. The global interactome (Figure 1) illustrates what should now be considered the anticipated complexity of CFTR interaction pathways facilitating normal function. It is important to emphasize that a number of interactors identified in the screen are currently under intense investigation and therefore provide important validation of the approach (Amaral, 2006; Guggino and Stanton, 2006). The relative importance of the many uncharacterized interactions, whether direct or indirect, remains to be elucidated. Intriguingly, we found that changes in the Hsp90 cochaperone folding environment markedly altered the stability and export of ΔF508 from the ER. This emphasizes the role of the folding environment in distinguishing between a mutation and a polymorphism, a result that has important implications for tissue-specific physiology and the correction of general misfolding disease. The CFTR interactome predicts that genetic modifiers that affect presentation of CF in the clinic (Cutting, 2005) are now likely to include a number of cellular components, in particular cellular chaperones that either directly or indirectly promote folding for export. We suggest the possibility that the folding capacity defined by Aha1 activity, and potentially other Hsc-Hsp40/70 regulators and Hsp90 cochaperones, is a likely target for therapeutic approaches using small molecular correctors or siRNA reagents.

Folding and Export of CFTR from the ER

Multiple lines of biochemical and biophysical evidence emphasize that folding of ΔF508 is kinetically impaired and that CFTR requires both interdomain and intradomain interactions to achieve the native state (Riordan, 2005). While the core cytosolic folding machinery components (Hsc-Hsp40/70 and Hsp90) were found in both wild-type and ΔF508 CFTR proteomes, Hsp90 cochaperones were most abundant in the ΔF508 CFTR proteome based on the number of recovered spectra, a measure of the robustness of the level of protein interactions (Liu et al., 2004). These results provide strong support for the interpretation that ΔF508 CFTR is kinetically trapped in an on-pathway, metastable folded state (or states) (Qu et al., 1997). As such, and as was previously observed, stalled intermediates in the ΔF508 folding pathway are likely targets for recruitment of components such as CHIP and the regulatory factors HspBP1 and Bag that bind the Hsc-Hsp70/40 complex and target CFTR to ERAD (Alberti et al., 2004; Dai et al., 2005; Meacham et al., 2001; Younger et al., 2006) (Figure 7A).

From the wealth of interactions observed in the CFTR interactome, we focused our attention on the molecular basis for the failure of ΔF508 to exit the ER. As has been observed in correction of amyloid disease (Johnson et al., 2005; Kelly and Balch, 2006), folding is the key event that needs to be understood if effective therapies are to be achieved. In addition to transient interactions with Hsc-Hsp70/40 complexes, we demonstrated that altered expression of the cochaperones p23 and FKBP8 can differentially affect stabilization of CFTR in the ER. p23, a cochaperone that can stabilize Hsp90-client interactions in the ATP state (Pratt and Toft, 2003), was found to be important to prevent destabilization and degradation of ΔF508. Thus, a decrease in p23 activity and, potentially, its interacting partner FKBP8 may lead to enhanced coupling to the Hsc-Hsp40/70 pathway and ERAD through HOP (Figure 7A).

In contrast to the apparent requirement for p23 and FKBP8 for controlling the stability of the band B glycoform of CFTR in the ER, siRNA reduction of Aha1, a cochaperone that is proposed to function as an Hsp90 ATPase activator (Harst et al., 2005; Lotz et al., 2003; Meyer, 2004; Panaretou et al., 2002), provided a new folding environment that favored ΔF508 export by the COPII export machinery (Stagg et al., 2006; Gurkan et al., 2006). Under these conditions, we have not detected a change in the total pools of Hsc-Hsp70 or BiP, indicating that it is unlikely that we induce a general stress response (Schroder and Kaufman, 2005) by siRNA reduction of Aha1. Similarly, we did not detect a change in the cellular levels of Hsp90, HOP, p23, FKBP8, or calnexin in response Aha1 siRNA, indicating that a change in expression of these cochaperones is not responsible for the observed effect of Aha1 reduction. Strikingly, in the presence of Aha1, the level of band C approached that observed for expression of Δ508 CFTR in temperature-corrected CFBE41o− cells. In this case, halide conductance was restored to a level, on average, that was equivalent to that found in the temperature-corrected CFBE41o− cell line. Our results suggest that even a modest change in the Hsp90 chaperone environment may be sufficient for long-term functional rescue of ΔF508 given that patients expressing low levels of functional CFTR display a mild disease phenotype (Welsh and Ostedgaard, 1998). This conclusion is also consistent with the widespread observation that ER stability and cell-surface availability of ΔF508 is highly variable between cell types in culture (Varga et al., 2004), likely reflecting differences in chaperone pools.

Energetics of Folding and Misfolding in the ER

Aha1 has been proposed to stimulate the ATPase of activity of Hsp90, thereby regulating the dynamics of chaperone-client interaction (Panaretou et al., 2002). Thus, our results with Aha1 suggest that energetic destabilization of the folding pathway by the Phe508 deletion leading to

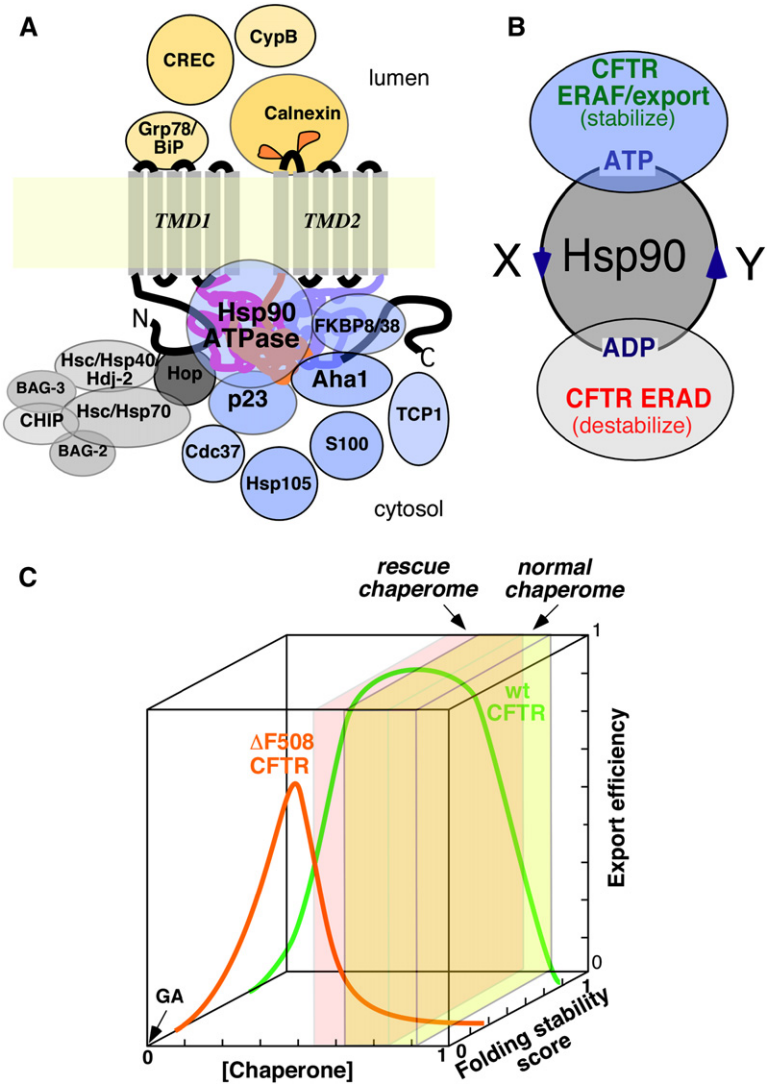

Figure 7. Hsp90 Chaperone/Cochaperone Interactions Directing CFTR Folding

(A) The cartoon highlights components involved in wild-type and ΔF508 CFTR folding. They consist of lumenal chaperones (yellow) and a two-state cytosolic system linked by HOP that consists of the Hsc-Hsp40/70 (gray) and Hsp90 (blue) chaperone complexes, which are regulated by a number of Hsc-Hsp70 (gray) and Hsp90 (blue) cochaperones. One or more of these protein interactions are kinetically disrupted by the Phe508 deletion, leading to disruption of the Hsc-Hsp70/Hsp90 chaperone-linked cycles and CF pathophysiology.

(B) Illustration of the potential role of Hsp90 and its cochaperones in folding and rescue of ΔF508 CFTR. The ATP/ADP cycle regulating folding for export through ERAF or targeting for ERAD can be dynamically controlled by cochaperone regulators (X and Y) to adjust the kinetics of the chaperone cycle to the kinetics and energetics of the folding pathway.

(C) A 3D plot illustrating the relationship between the (co)chaperone concentration in the cytosol (x axis), a hypothetical "folding stability score" defined by global protein energetics (Sekijima et al., 2005) (z axis), and "export efficiency" reflecting the level of transport to the cell surface (y axis). Whereas the more energetically stable wild-type CFTR (green curve) responds to the folding activity of the CFTR chaperome at the normal concentration of Aha1 (yellow box, "normal chaperome"), the reduced folding energetics of ΔF508 (orange curve), being outside the normal chaperome pool, favors misfolding and targeting for degradation. A change in Hsp90 cycling afforded by modest downregulation of Aha1 (pink box partially overlapping with normal chaperome, "rescue chaperome") provides a more productive solvent (Kelly and Balch, 2006) for the folding of ΔF508, promoting export. The overlap region (beige box) of the normal and rescue chaperome pools in this situation may retain full functionality of the wild-type CFTR fold and other cellular components given their more robust folding energetics. Geldanamycin (GA; lower left corner), an Hsp90 inhibitor, blocks both wild-type and ΔF508 CFTR folding and export by directly binding to Hsp90 and arresting the folding cycle in the ADP state (Loo et al., 1998).

poor export and enhanced degradation of the ΔF508 mutant may be kinetically uncoupled from the normal regulated ATPase activity of the Hsp90-dependent client folding cycle. The availability of chaperones and cochaperones for folding of cargo will be sensitive to the global cellular pool that we now define as the chaperome, a general term to define the unique steady-state composition of chaperones and their regulators in a given cell type. It is well established that the chaperome can be altered by multiple signaling pathways to accommodate cellular stress and misfolding load. By modulating the chaperome through siRNA or overexpression as shown herein, we altered the dynamic relationship between those chaperone components specifically required for folding of CFTR. As a cargo-specific collection of chaperome components (the CFTR chaperome), it is now apparent that, while the steady-state balance of the folding components in the cell required for the CFTR chaperome likely defines the success or failure of the wild-type fold, it can be adjusted to modulate the success or failure of the ΔF508 mutant fold for export.

The capacity of the cellular chaperome to specifically facilitate protein folding is consistent with recent observations that chaperones regulate specific cellular protein folding pathways (Albanese et al., 2006) rather than simply functioning as inhibitors of protein aggregation. Moreover, recent studies now directly show that the GroEL-GroES chaperonin cage complex provides a physical environment optimized to catalyze protein assembly (Tang et al., 2006). The Hsp90 chaperone complex could be viewed in a similar vein, despite its assembly state being more dynamic and flexible in composition. As illustrated

in Figure 7B, our results now raise the possibility that a modified CFTR-Hsp90 chaperone complex defined by reduced levels of Aha1 favors ΔF508 folding in a fashion that supports stabilization from ERAD pathways and directs coupling to the ER export machinery. One possibility is that reduction of Hsp90 cycling in response to reduced Aha1 activity might allow additional time for the kinetically challenged ΔF508 mutant to a achieve a more export-competent fold and mature to an Hsp90-dependent step required for coupling to the COPII ER export machinery. This conclusion is consistent with the observation that Aha1 reduced the steady-state level of Hsp90 bound to ΔF508. Thus, an ordered folding pathway linked to the intrinsic energetics of the wild-type or mutant CFTR fold might be coordinated with the Hsp90 ATPase cycle. These results, when combined with the effects of p23 and FKBP8, suggest that Hsp90 cochaperone component activities are likely integrated. This may differ substantially between cell types and therefore may be differentially sensitive to specific Aha1 modulation.

To help visualize the complex relationships between folding energetics, the chaperome, and export machineries (Kelly and Balch, 2006), we can now arbitrarily assign a "folding stability score" to wild-type and mutant CFTR folding pathways (Sekijima et al., 2005). The folding stability score (Figure 7C, z axis) reflects both the kinetic and thermodynamic properties of the CFTR fold. For wild-type CFTR, this is illustrated as the green curve in Figure 7C. Folding of wild-type CFTR is likely evolutionarily optimized relative to the normal cellular chaperome, illustrated as the yellow box in Figure 7C. This chaperome would therefore support efficient folding for export. In contrast, the energetically destabilized ΔF508 variant, illustrated as the orange curve in Figure 7C, is defective in export from the ER because its folding energetics lie outside the capacity of the normal Hsp90-dependent chaperone environment to promote folding, resulting in targeting for ERAD through Hsc-Hsp40/70-mediated pathways. However, an alteration in the activity of Aha1 and potentially other cochaperones can provide new capacity to the cellular chaperome to create a CFTR "rescue chaperome" that can support folding and export, illustrated as the pink box overlapping with the yellow normal chaperone pool in Figure 7C. We suggest that the inability of a variant protein to achieve a more native (functional) fold in response to a particular cellular chaperome is a general feature of conformational diseases (Moyer and Balch, 2001; Ulloa-Aguirre et al., 2004) that can be altered by adjusting its composition. Thus, the chaperone environment can dictate the difference between a deleterious mutation and a tolerated polymorphism. This is consistent with recent results showing that global alteration of Ins2- and HSF1-mediated stress-response pathways arrest and reverse onset of aggressive misfolding amyloid diseases in *C. elegans* (Gidalevitz et al., 2006; Morley and Morimoto, 2004). While we have focused on CFTR folding and ER export, knowledge of the global interactome (Figure 1) provides an initial roadmap to explore more completely CFTR folding, trafficking, and function in health and human disease.

EXPERIMENTAL PROCEDURES

Immunoprecipitation

CFTR and coimmunoprecipitated proteins in whole-cell detergent lysates were bound to Sepharose beads coupled with the anti-CFTR monoclonal antibody M3A7 as described in detail in the Supplemental Experimental Procedures.

Digestion of Protein Complexes of CFTR for MudPIT

Following immunoprecipitation, protein complexes were digested and subjected to LC/LC-MS/MS analysis using MudPIT, and tandem mass spectra were analyzed sequentially and annotated as described in detail in the Supplemental Experimental Procedures.

siRNA and Overexpression

siRNA solutions were prepared by mixing serum and antibiotic-free DMEM or MEM-α with the indicated siRNA at a working concentration of 0.6 μM human p23 (Ambion, Austin, TX, USA, catalog #16704 ID 18391), 0.6 μM human FKBP8 (Ambion, catalog #16704 ID 45182), or 2 μM human Aha1 using 1 μM each of two siRNAs (Dharmacon, Lafayette, CO, USA) directed to hAha1 sequences ATTGGTCCACG GATAAGCT and GTGAGTAAGCTTGATGGAG and 6 μl of HiPerFect (QIAGEN, Valencia, CA, USA) per well of a 12-well dish. Control siRNA (Dharmacon, catalog #CONJB-000015) was added at a concentration equal to p23, FKBP8, and Aha1 siRNA in each experiment. The siRNA mixture was added to cells and cells were cultured as described in detail in the Supplemental Experimental Procedures. Overexpression was performed as previously described (Wang et al., 2004). SDS-PAGE and immunoblotting were performed as described in the Supplemental Experimental Procedures.

Iodide Efflux Assay

The detailed protocol used for the iodide flux assay is described in the Supplemental Experimental Procedures.

Supplemental Data

Supplemental Data include Supplemental Discussion, Supplemental Experimental Procedures, Supplemental References, seven tables, and four figures and can be found with this article online at http://www.cell.com/cgi/content/full/127/4/803/DC1/.

ACKNOWLEDGMENTS

This work was supported by NIH grants GM42336 to W.E.B., DK51870 to J.R.R., GM78654 to J.W.K., and GM45678/NIH RR11823 to J.R.Y. J.V., X.W., P.L., A.V.K., and D.M.H. were supported by fellowships from the Cystic Fibrosis Foundation (CFF) and funding from the Cystic Fibrosis Consortium (CFC). Support to J.R.Y. for instrumentation for mass spectrometry was provided by the CFF and CFC. We thank Dr. N. Bradbury at the University of Pittsburgh School of Medicine for HEK293 cells stably expressing wild-type and ΔF508 CFTR, Dr. J. Clancy at the University of Alabama at Birmingham for the CFBE41o− and corrected CFBE41o− (HBE) cell lines, Dr. D. Smith at the Mayo Clinic (Scottsdale, AZ, USA) for the JJ3 antibody to p23, and Dr. K. Nakayama at Kyushu University (Fukuoka, Japan) for FKBP8-specific antibody. This is TSRI manuscript #16775-CB.

Received: April 8, 2006
Revised: July 8, 2006
Accepted: September 11, 2006
Published: November 16, 2006

REFERENCES

Albanese, V., Yam, A.Y., Baughman, J., Parnot, C., and Frydman, J. (2006). Systems analyses reveal two chaperone networks with distinct functions in eukaryotic cells. Cell *124*, 75–88.

Alberti, S., Bohse, K., Arndt, V., Schmitz, A., and Hohfeld, J. (2004). The cochaperone HspBP1 inhibits the CHIP ubiquitin ligase and stimulates the maturation of the cystic fibrosis transmembrane conductance regulator. Mol. Biol. Cell *15*, 4003–4010.

Amaral, M.D. (2006). Therapy through chaperones: Sense or antisense? Cystic fibrosis as a model disease. J. Inherit. Metab. Dis. *29*, 477–487.

Cutting, G.R. (2005). Modifier genetics: cystic fibrosis. Annu. Rev. Genomics Hum. Genet. *6*, 237–260.

Dai, Q., Qian, S.B., Li, H.H., McDonough, H., Borchers, C., Huang, D., Takayama, S., Younger, J.M., Ren, H.Y., Cyr, D.M., et al. (2005). Regulation of the cytoplasmic quality control protein degradation pathway by BAG2. J. Biol. Chem. *280*, 38673–38681.

Gidalevitz, T., Ben-Zvi, A., Ho, K.H., Brignull, H.R., and Morimoto, R.I. (2006). Progressive disruption of cellular protein folding in models of polyglutamine diseases. Science *311*, 1471–1474.

Guggino, W.B., and Stanton, B.A. (2006). New insights into cystic fibrosis: molecular switches that regulate CFTR. Nat. Rev. Mol. Cell Biol. *7*, 426–436.

Gurkan, C., Stagg, S.M., Lapointe, P., and Balch, W.E. (2006). The COPII cage: unifying principles of vesicle coat assembly. Nat. Rev. Mol. Cell Biol. *7*, 727–738.

Harst, A., Lin, H., and Obermann, W.M. (2005). Aha1 competes with Hop, p50 and p23 for binding to the molecular chaperone Hsp90 and contributes to kinase and hormone receptor activation. Biochem. J. *387*, 789–796.

Johnson, S.M., Wiseman, R.L., Sekijima, Y., Green, N.S., Adamski-Werner, S.L., and Kelly, J.W. (2005). Native state kinetic stabilization as a strategy to ameliorate protein misfolding diseases: a focus on the transthyretin amyloidoses. Acc. Chem. Res. *38*, 911–921.

Kelly, J.W., and Balch, W.E. (2006). The integration of cell and chemical biology in protein folding. Nat. Chem. Biol. *2*, 224–227.

Lee, M.C., Miller, E.A., Goldberg, J., Orci, L., and Schekman, R. (2004). Bi-directional protein transport between the ER and Golgi. Annu. Rev. Cell Dev. Biol. *20*, 87–123.

Lewis, H.A., Buchanan, S.G., Burley, S.K., Conners, K., Dickey, M., Dorwart, M., Fowler, R., Gao, X., Guggino, W.B., Hendrickson, W.A., et al. (2004). Structure of nucleotide-binding domain 1 of the cystic fibrosis transmembrane conductance regulator. EMBO J. *23*, 282–293.

Liu, H., Sadygov, R.G., and Yates, J.R., 3rd. (2004). A model for random sampling and estimation of relative protein abundance in shotgun proteomics. Anal. Chem. *76*, 4193–4201.

Loo, M.A., Jensen, T.J., Cui, L., Hou, Y., Chang, X.B., and Riordan, J.R. (1998). Perturbation of Hsp90 interaction with nascent CFTR prevents its maturation and accelerates its degradation by the proteasome. EMBO J. *17*, 6879–6887.

Lotz, G.P., Lin, H., Harst, A., and Obermann, W.M. (2003). Aha1 binds to the middle domain of Hsp90, contributes to client protein activation, and stimulates the ATPase activity of the molecular chaperone. J. Biol. Chem. *278*, 17228–17235.

Meacham, G.C., Patterson, C., Zhang, W., Younger, J.M., and Cyr, D.M. (2001). The Hsc70 co-chaperone CHIP targets immature CFTR for proteasomal degradation. Nat. Cell Biol. *3*, 100–105.

Meyer, P. (2004). Structural basis for recruitment of the ATPase activator Aha1 to the Hsp90 chaperone machinery. EMBO J. *23*, 1402–1410.

Morley, J.F., and Morimoto, R.I. (2004). Regulation of longevity in Caenorhabditis elegans by heat shock factor and molecular chaperones. Mol. Biol. Cell *15*, 657–664.

Moyer, B.D., and Balch, W.E. (2001). A new frontier in pharmacology: the endoplasmic reticulum as a regulated export pathway in health and disease. Expert Opin. Ther. Targets *5*, 165–176.

Nielsen, J.V., Mitchelmore, C., Pedersen, K.M., Kjaerulff, K.M., Finsen, B., and Jensen, N.A. (2004). Fkbp8: novel isoforms, genomic organization, and characterization of a forebrain promoter in transgenic mice. Genomics *83*, 181–192.

Nishikawa, S., Brodsky, J.L., and Nakatsukasa, K. (2005). Roles of molecular chaperones in endoplasmic reticulum (ER) quality control and ER-associated degradation (ERAD). J. Biochem. (Tokyo) *137*, 551–555.

Panaretou, B., Siligardi, G., Meyer, P., Maloney, A., Sullivan, J.K., Singh, S., Millson, S.H., Clarke, P.A., Naaby-Hansen, S., Stein, R., et al. (2002). Activation of the ATPase activity of Hsp90 by the stress-regulated co-chaperone Aha1. Mol. Cell *10*, 1307–1318.

Pratt, W.B., and Toft, D.O. (2003). Regulation of signaling protein function and trafficking by the hsp90/hsp70-based chaperone machinery. Exp. Biol. Med. (Maywood) *228*, 111–133.

Qu, B.H., Strickland, E.H., and Thomas, P.J. (1997). Localization and suppression of a kinetic defect in cystic fibrosis transmembrane conductance regulator folding. J. Biol. Chem. *272*, 15739–15744.

Riordan, J.R. (2005). Assembly of functional CFTR chloride channels. Annu. Rev. Physiol. *67*, 701–718.

Schroder, M., and Kaufman, R.J. (2005). The mammalian unfolded protein response. Annu. Rev. Biochem. *74*, 739–789.

Sekijima, Y., Wiseman, R.L., Matteson, J., Hammarstrom, P., Miller, S.R., Sawkar, A.R., Balch, W.E., and Kelly, J.W. (2005). The biological and chemical basis for tissue-selective amyloid disease. Cell *121*, 73–85.

Shirane, M., and Nakayama, K.I. (2003). Inherent calcineurin inhibitor FKBP38 targets Bcl-2 to mitochondria and inhibits apoptosis. Nat. Cell Biol. *5*, 28–37.

Stagg, S.M., Gurkan, C., Fowler, D.M., LaPointe, P., Foss, T.R., Potter, C.S., Carragher, B., and Balch, W.E. (2006). Structure of the Sec13/31 COPII coat cage. Nature *439*, 234–238.

Tang, Y.C., Chang, H.C., Roeben, A., Wischnewski, D., Wischnewski, N., Kerner, M.J., Hartl, F.U., and Hayer-Hartl, M. (2006). Structural features of the GroEL-GroES nano-cage required for rapid folding of encapsulated protein. Cell *125*, 903–914.

Ulloa-Aguirre, A., Janovick, J.A., Brothers, S.P., and Conn, P.M. (2004). Pharmacologic rescue of conformationally-defective proteins: implications for the treatment of human disease. Traffic *5*, 821–837.

Varga, K., Jurkuvenaite, A., Wakefield, J., Hong, J.S., Guimbellot, J.S., Venglarik, C.J., Niraj, A., Mazur, M., Sorscher, E.J., Collawn, J.F., et al. (2004). Efficient intracellular processing of the endogenous cystic fibrosis transmembrane conductance regulator in epithelial cell lines. J. Biol. Chem. *279*, 22578–22584.

Wang, X., Matteson, J., An, Y., Moyer, B., Yoo, J.S., Bannykh, S., Wilson, I.A., Riordan, J.R., and Balch, W.E. (2004). COPII-dependent export of cystic fibrosis transmembrane conductance regulator from the ER uses a di-acidic exit code. J. Cell Biol. *167*, 65–74.

Washburn, M.P., Wolters, D., and Yates, J.R., 3rd. (2001). Large-scale analysis of the yeast proteome by multidimensional protein identification technology. Nat. Biotechnol. *19*, 242–247.

Wegele, H., Muller, L., and Buchner, J. (2004). Hsp70 and Hsp90 a relay team for protein folding. Rev. Physiol. Biochem. Pharmacol. *151*, 1–44.

Welsh, M.J., and Ostedgaard, L.S. (1998). Cystic fibrosis problem probed by proteolysis. Nat. Struct. Biol. *5*, 167–169.

Young, J.C., Barral, J.M., and Ulrich Hartl, F. (2003). More than folding: localized functions of cytosolic chaperones. Trends Biochem. Sci. *28*, 541–547.

Younger, J.M., Chen, L., Ren, H.Y., Rosser, M.F., Turnbull, E.L., Fan, C.Y., Patterson, C., and Cyr, D.M. (2006). Sequential quality-control checkpoints triage misfolded cystic fibrosis transmembrane conductance regulator. Cell *126*, 571–582.